Molecular Modeling Connect
ISSN: 3006-9084
2025, Article ID. 2025.0005, Cite as: https://www.doi.org/10.69709/MolModC.2025.339955

SCIFINITI

Research Article

OPEN ACCESS

Smart Gas Sensing by (Al/C/Si)-Doped Boron Nitride Nanomaterial Towards Grabbing Nitric Oxide: A Novel Applied Technique for Air Pollution Reduction by DFT Analysis

Fatemeh Mollaamin[✉,1]

[1] Department of Biomedical Engineering, Faculty of Engineering and Architecture, Kastamonu University, Kastamonu 37150, Turkey

Article History
Submitted: August 21, 2024 Accepted: December 9, 2024 Published: April 4, 2025

Abstract
The electronic, magnetic, and thermodynamic properties of adsorption of toxic gases, including Nitric oxide (NO) by using Y (Y = Al, C, Si)-doped boron nitride nanocage (BN) have been investigated using density functional theory (DFT). The results denote that NO→Y–BN are stable compounds, with the most stable adsorption site being the center of the cage ring. Furthermore, the reported results of nuclear magnetic resonance (NMR) spectroscopy have exhibited the strength of covalent bonds between aluminum, carbon, silicon, and NO molecules toward toxic gas removal from the air. Based on the results of ΔG^{o}_{ads} amounts in this research, the maximum efficiency of Al, C, and Si atoms doping of BN for gas molecules adsorption depends on the covalent bond between NO molecules and Y–BN as a potent sensor for air pollution removal. Finally, the high selectivity of atom-doped boron nitride nanocage (gas sensor) for gas molecule adsorption has resulted in: Al > C > Si.

Keywords:
air pollution; gas sensor; doping; boron nitride (BN); density functional theory (DFT)

1. Introduction

Developing non-carbon-based adsorbents is essential for removing heavy metals from post-incineration flue gas. Boron nitride nanomaterials have been used due to their unparalleled eco-friendly attributes, making them ideal for pollutant adsorption and semiconducting properties [1–4]. Boron nitride nanomaterials usually exhibit semi-leading behavior, which is considered a proper alternative to carbon nanotubes. The properties of boron and nitrogen atoms, which are the first neighbors of carbon in the periodic table, make boron nitride an interesting subject of numerous studies [5–7].

In recent years, different investigations on the adsorption of chemical contaminants and the application of various boron nitride nanostructures as adsorbents for water purification have been studied [8–10].

Various physical shapes of boron nitride (BN)-based nano adsorbents such as nanoparticles, fullerenes, nanotubes, nanofibers, nanoribbons, nanosheets, nanomeshes, nanoflowers, and hollow spheres have been broadly considered possible adsorbents. They are valued for their exceptional characteristics, including a large surface area, structural variability, high chemical/mechanical strength, abundant structural defects, high reactive sites, and functional groups [11,12].

Regarding computational methods, the researchers have investigated the structural stability and physicochemical properties of the N-rich BN fullerene using the density functional theory at the level of the generalized gradient approximation. For this purpose, the Heyd–Scuseria–Ernzerhof (HSE) screened hybrid density functional and the 6-31G(d) basis set was used. They have indicated that

Corresponding Author:
Fatemeh Mollaamin, Department of Biomedical Engineering, Faculty of Engineering and Architecture, Kastamonu University, Kastamonu 37150, Turkey, fmollaamin@kastamonu.edu.tr

© 2025 Copyright by the Author.
Licensed as an open access article using a CC BY 4.0 license.

the $B_{24}N_{36}$ fullerene is stable and behaves as a semiconductor compound [13].

The capability to control the physical and chemical properties of nanosized materials utilizing experimental and theoretical methods has impacted positively many research fields [14–18].

Therefore, in this research article, a computational study of NO adsorption on the surface of a non-symmetric atom-doped boron nitride was reported. The effect of NO adsorption on the structural and physicochemical properties has been determined, and the possibility of using this nanostructure for applications in gas sensing has been discussed. Our findings can divulge the promising potential of the doped (BN) -based nanomaterial as a highly sensitive molecular sensor for NO detection and a catalyst for NO dissociation.

2. Computation towards Materials Modeling

The BN hollow nanocages have typically spherical morphologies with crystalline structures. Their internal space is divided into separate compartments by the internal walls. This method may be generally applicable to the fabrication of BN-sheathed nanocrystals (Figure 1).

The input Z-matrix for adsorption of NO molecules in air by the Y–BN has been designed using 6-311+G (d,p), EPR–3, LANL2DZ basis set. In this study, the interaction between gas molecules and Y–BN was modeled and analyzed [19–35] (Figure 2).

3. Materials & Methods

In our previous works, the application of density functional theory (DFT) calculations through materials modelling has been accomplished [36–59]. The first principle's calculations assess an important function in developing and optimizing new energy-saving and conversion materials [60].

In DFT, as it is used for computational chemistry, the hybrid functional Becke 3-parameter Lee-Yang-Parr (B3LYP) [27] appears to offer the greatest contribution. A new hybrid exchange–correlation function named the Coulomb-Attenuating Method with B3LYP (CAM–B3LYP) is proposed, which combines the hybrid qualities of B3LYP and the long-range correction [61]. Besides, in the DFT–D3 method of Grimme et al., the following expression for the Van Der Waals (vdW)-dispersion energy-correction term is used [62].

4. Results and Discussion

The data has evaluated the efficiency of a boron nitride nanocage doped with aluminum, carbon, and silicon (Y–BN) for gas detection. The nuclear quadrupole resonance (NQR) frequency at which transitions occur is particular for NO→Y–BN complexes (Table 1) [63–66]. In this research, the electric potential has been evaluated for NO→Al–BN, NO→C–BN, and NO→Si–BN complexes (Table 1). This is considered as the amount of work energy required to transfer an electric charge from one position to another within the electric field.

The doping atoms of "Al (15), C (15), Si (15)" on the BN have shown the most potential for accepting the electron from the electron donor of "N (1) in NO" adsorbed on the BN (Table 1). Furthermore, the electric potential of nuclear quadrupole resonance for some atoms of "Al, C, Si/ B, N in Y– BN and N, O" of gas molecules has been sketched (Figure 3a–c).

In Figure 3a,b, the behavior of NO adsorption on the Al–BN, and C–BN, respectively, was observed with high sensitivity based on the relation coefficient of $R^2 = 0.9945$ and $R^2 = 0.9827$. The adsorption of NO molecules on the Si–BN in Figure 3c has illustrated the analogous with the highest sensing of $R^2 = 0.9925$. The curve of Y–BN is waved by these gas molecules. The fluctuated peaks for electric potential have been shown around NO trapping on the Y–BN, which demonstrates the electron-accepting specifications of nitrogen and oxygen versus the aluminum, carbon, and silicon doped on the BN (Figure 3a–c). Aluminum and silicon doped on BN (adsorbents) with an average of 1.1 coulomb of atomic charge on (Al, Si)–BN have shown similar behavior in the procedure of gas molecules (adsorbates) removal. "The NMR data of isotropic (σ_{iso}) and anisotropic shielding tensors (σ_{aniso})" [64,65] of gas molecules trapped in the "Y–BN" towards the formation of "NO→Al–BN, NO→C–BN, and NO→Si–BN" complexes have been computed by "Gaussian 16 revision C.01" program package [34] and been shown in Table 2.

The adsorption of NO molecules can introduce spin polarization on the Y–BN, which indicates that these surfaces might be applied as magnetic scavenging surfaces for a gas detector. Figure 4 exhibited the same tendency of shielding for boron and nitrogen; however, a considerable deviation exists from doping atoms of Al (15), C (15), and Si (15).

In Figure 4a–c, gas molecules of NO molecules in the complexes of NO→C–BN (Figure 4a), NO→Si–BN (Figure 4b), and NO→Al–BN (Figure 4c) denote the fluctuation in the chemical shielding during ion trapping. Figure 4a–c shows the gap in chemical shielding between

2025, Vol. 1, Article ID. 2025.0005
https://www.doi.org/10.69709/MolModC.2025.339955

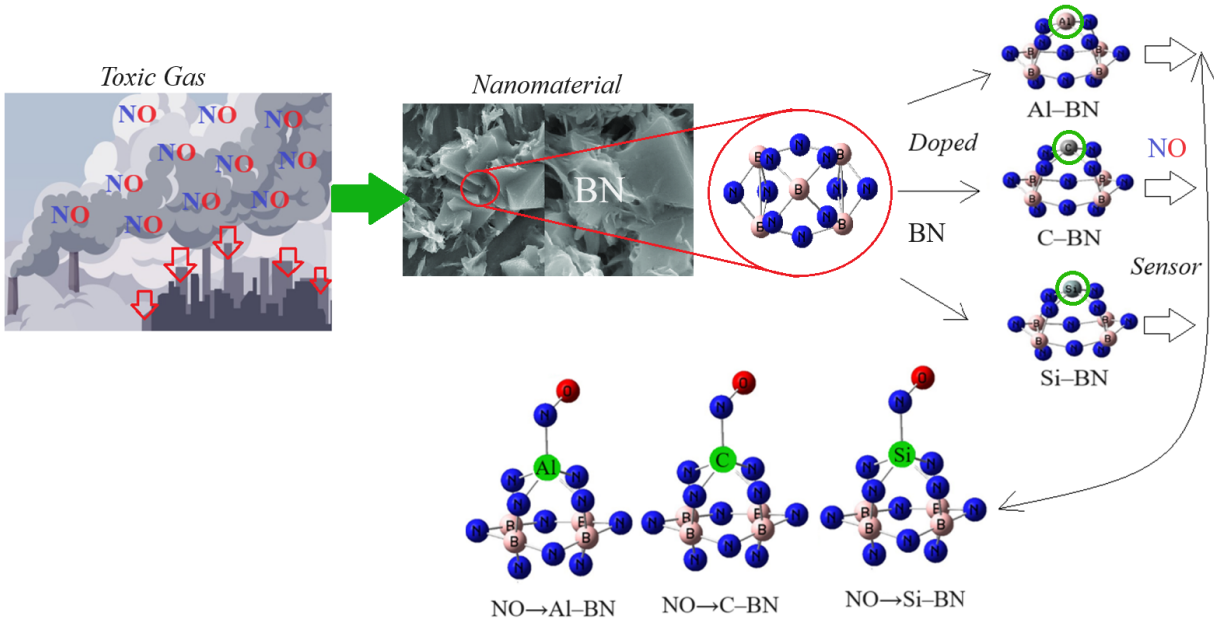


Figure 1: Application of Y–BN towards adsorption of gas molecules of NO and formation of complexes: NO→Al–BN, NO→C–BN, and NO→Si–BN.

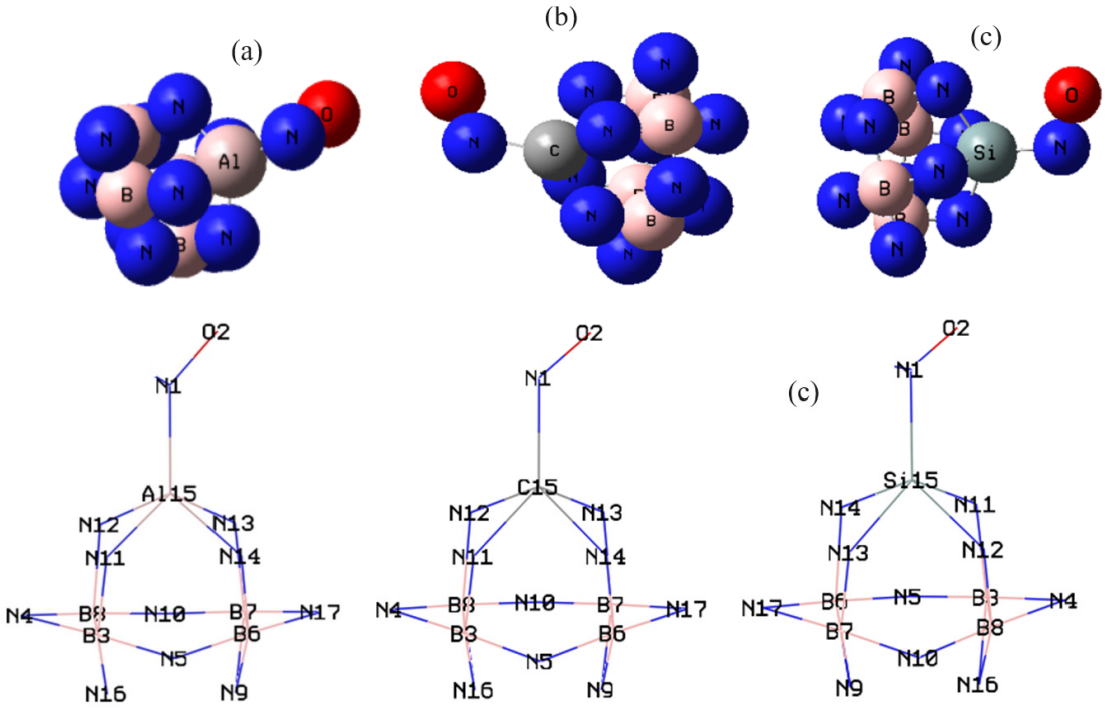


Figure 2: Optimized structures of (**a**) NO→Al–BN, (**b**) NO→C–BN, and (**c**) NO→Si–BN using CAM–B3LYP–D3/6-311+G (d,p), LANL2DZ calculation.

aluminum, carbon, and silicon doping of Y–BN nanocage, and gas molecules. The yield of electron-accepting for doping atoms on the Y–BN through gas molecules adsorption can be ordered as: Si > Al >> C approves the possibility of a covalent bond between aluminum, carbon, silicon, and these NO molecules.

The several clusters containing NO→Al–BN (Figure 5a), NO→C–BN (Figure 5b), and NO→Si–BN (Figure 5c) have been computed by Gaussian 16 revision

Table 1: The electric potential (E_p/a.u.) and Bader charge (Q/coulomb) through NQR calculation for NO→Al–BN, NO→C–BN, and NO→Si–BN complexes using CAM–B3LYP–D3/EPR–3, LANL2DZ calculation.

NO→Al–BN			NO→C–BN			NO→Si–BN		
Atom	**Q**	**E_p**	**Atom**	**Q**	**E_p**	**Atom**	**Q**	**E_p**
N1	−0.1853	−18.082	N1	0.1466	−18.1839	N1	−0.1906	−18.2495
O2	−0.0268	−21.9319	O2	−0.0949	−22.2001	O2	−0.0846	−22.2135
B3	0.3040	−11.2292	B3	0.0321	−11.2869	B3	0.0273	−11.2791
N4	−0.1757	−18.0903	N4	−0.014	−18.2911	N4	0.0080	−18.2831
N5	−0.1524	−18.0544	N5	−0.0458	−18.268	N5	0.0060	−18.2656
B6	0.3033	−11.2288	B6	0.0310	−11.2865	B6	0.0310	−11.2787
B7	0.2954	−11.2274	B7	0.0323	−11.2871	B7	0.0303	−11.2793
B8	0.2970	−11.2278	B8	0.0316	−11.287	B8	0.0316	−11.2788
N9	−0.1558	−18.0628	N9	−0.0256	−18.2799	N9	−0.0205	−18.269
N10	−0.1434	−18.0452	N10	−0.0447	−18.2682	N10	0.0066	−18.2652
N11	−0.2581	−18.1141	N11	−0.0369	−18.2631	N11	−0.2401	−18.2808
N12	−0.2549	−18.1122	N12	−0.0337	−18.2633	N12	−0.2300	−18.2805
N13	−0.2532	−18.1122	N13	−0.0326	−18.2642	N13	−0.2316	−18.2817
N14	−0.2595	−18.1145	N14	−0.0328	−18.2626	N14	−0.2309	−18.2802
Al15	0.9984	−43.644	C15	0.1190	−14.5472	Si15	1.0996	−1.75968
N16	−0.1580	−18.0648	N16	−0.0259	−18.2804	N16	−0.0204	−18.2692
N17	−0.1748	−18.0893	N17	−0.0091	−18.2903	N17	0.0082	−18.2832

Table 2: Data of NMR shielding tensors for selected atoms of NO→Al–BN, NO→C–BN, and NO→Si–BN.

NO→Al–BN			NO→C–BN			NO→Si–BN		
Atom	**σ_{iso}**	**σ_{aniso}**	**Atom**	**σ_{iso}**	**σ_{aniso}**	**Atom**	**σ_{iso}**	**σ_{aniso}**
N1	8623.32	27621.57	N1	767.22	574.98	N1	192.56	384.90
O2	19,114.01	60055.67	O2	1697.96	1904.72	O2	483.66	446.82
B3	86.22	111.56	B3	83.21	75.50	B3	82.97	83.28
N4	398.76	5613.57	N4	698.49	846.36	N4	632.16	715.69
N5	1776.02	4560.20	N5	419.17	284.09	N5	460.89	248.70
B6	49.90	132.42	B6	84.90	76.89	B6	82.84	84.06
B7	88.70	112.26	B7	83.80	78.10	B7	83.55	82.75
B8	71.25	98.23	B8	84.84	75.04	B8	82.66	83.30
N9	673.90	3914.01	N9	421.55	778.5	N9	336.67	513.56
N10	2101.53	4479.16	N10	417.63	182.60	N10	457.73	296.56
N11	1145.30	6048.66	N11	574.52	402.81	N11	461.37	425.06
N12	284.26	4440.80	N12	538.46	433.46	N12	468.95	388.36
N13	434.51	1761.12	N13	581.63	365.00	N13	499.78	451.39
N14	681.36	2664.93	N14	556.56	519.43	N14	465.66	387.06
Al15	44.57	1469.07	C15	8.39	43.65	Si15	14.62	12.52
N16	496.25	2696.81	N16	390.13	810.91	N16	329.86	536.87
N17	2319.99	5536.37	N17	685.03	860.42	N17	611.84	711.69

C.01 program package [34] towards extracting IR spectra from GaussView 6.1 [35].

Table 3, through the thermodynamic specifications, concluded that Y–BN, due to the adsorption of NO molecules, might be more efficient sensors for detecting and removing the gas molecules from polluted air.

It has been shown that for a given number of nitrogen donor sites in NO molecules, the stabilities of complexes owing to doping atoms of Al, C, and Si can be considered as: NO→Al–BN > NO→C–BN > NO→Si–BN (Table 3).

The thermodynamic data in Table 3 could detect the maximum efficiency of Al, C, and Si atoms doping of BN for gas molecules adsorption through ΔG^o_R which depends on the covalent bond between NO molecules and Y–BN as a potent sensor for air pollution removal. The adsorption process of NO molecules on the Y–BN is affirmed by the ΔG^o_R quantities: $\Delta G^o_{ads} = \Delta G^o_{NO\rightarrow Y-BN} - (\Delta G^o_{NO} + \Delta G^o_{Y-BN})$; Y = Al, C, Si.

2025, Vol. 1, Article ID. 2025.0005
https://www.doi.org/10.69709/MolModC.2025.339955

Table 3: The thermodynamic characteristics of NO→Al–BN, NO→C–BN, and NO→Si–BN complexes.

Compound	Dipole moment (Debye)	$\Delta E^o \times 10^{-3}$ (kcal/mol)	$\Delta H^o \times 10^{-3}$ (kcal/mol)	$\Delta G^o \times 10^{-3}$ (kcal/mol)	S^o (cal/K.mol)
NO→Al–BN	0.6009	−630.889	−630.889	−630.920	103.437
NO→C–BN	0.2465	−510.557	−510.556	−510.588	103.732
NO→Si–BN	1.1293	−489.207	−489.206	−489.239	108.794

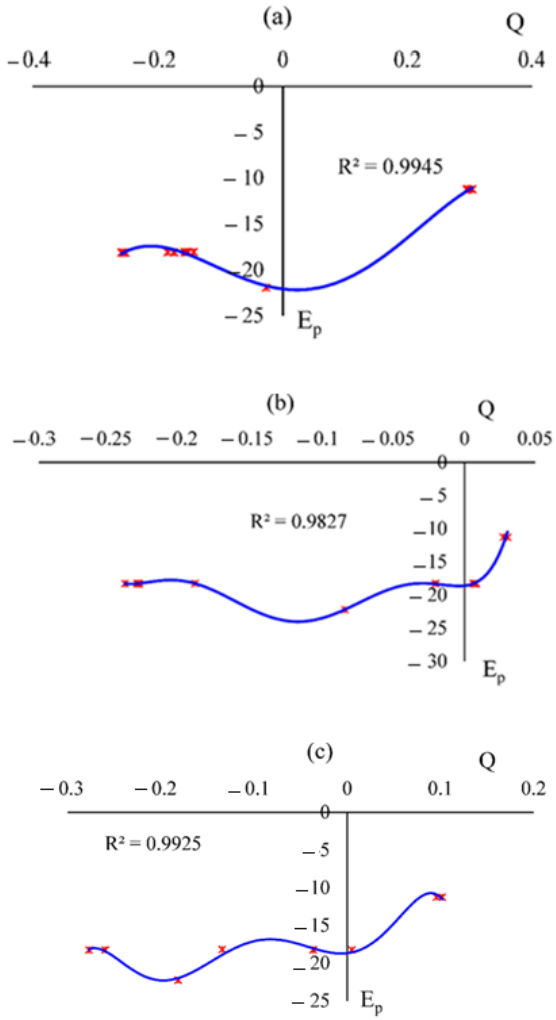


Figure 3: Electric potential (E_p/a.u.) versus Bader charge (Q/coulomb) through NQR calculation for (**a**) NO→Al–BN, (**b**) NO→C–BN, and (**c**) NO→Si–BN complexes.

5. Conclusions

This research has investigated doping of Al, C, and Si elements on the boron nitride nanocage (Y–BN) for enhancing toxic gas sensing of these nanomaterials for air pollution removal. Therefore, no molecular separation involving Y–BN has been experimentally conducted based on electrostatic interactions between the gas molecules and Y–BN. The selectivity of atom-doped on boron nitride nanocage (gas sensor) for gas molecule adsorption can result in: C–BN and Si–BN for NO adsorption.

List of Abbreviations

NO	Nitric Oxide
BN	Boron Nitride
DFT	Density Functional Theory
NMR	Nuclear Magnetic Resonance
B3LYP	Becke 3-parameter Lee-Yang-Parr
CAM	Coulomb-Attenuating Method
NQR	Nuclear Quadrupole Resonance

Author Contributions

The author confirms that she was solely responsible for the conception, design, analysis, interpretation, drafting, and final approval of the article.

Availability of Data and Materials

Data supporting the results of this study are available upon request from the corresponding author.

Conflicts of Interest

The author declares no conflicts of interest regarding this manuscript.

Funding

The research has no external funding support.

Acknowledgments

The author is grateful to Kastamonu University for completing this paper and its research.

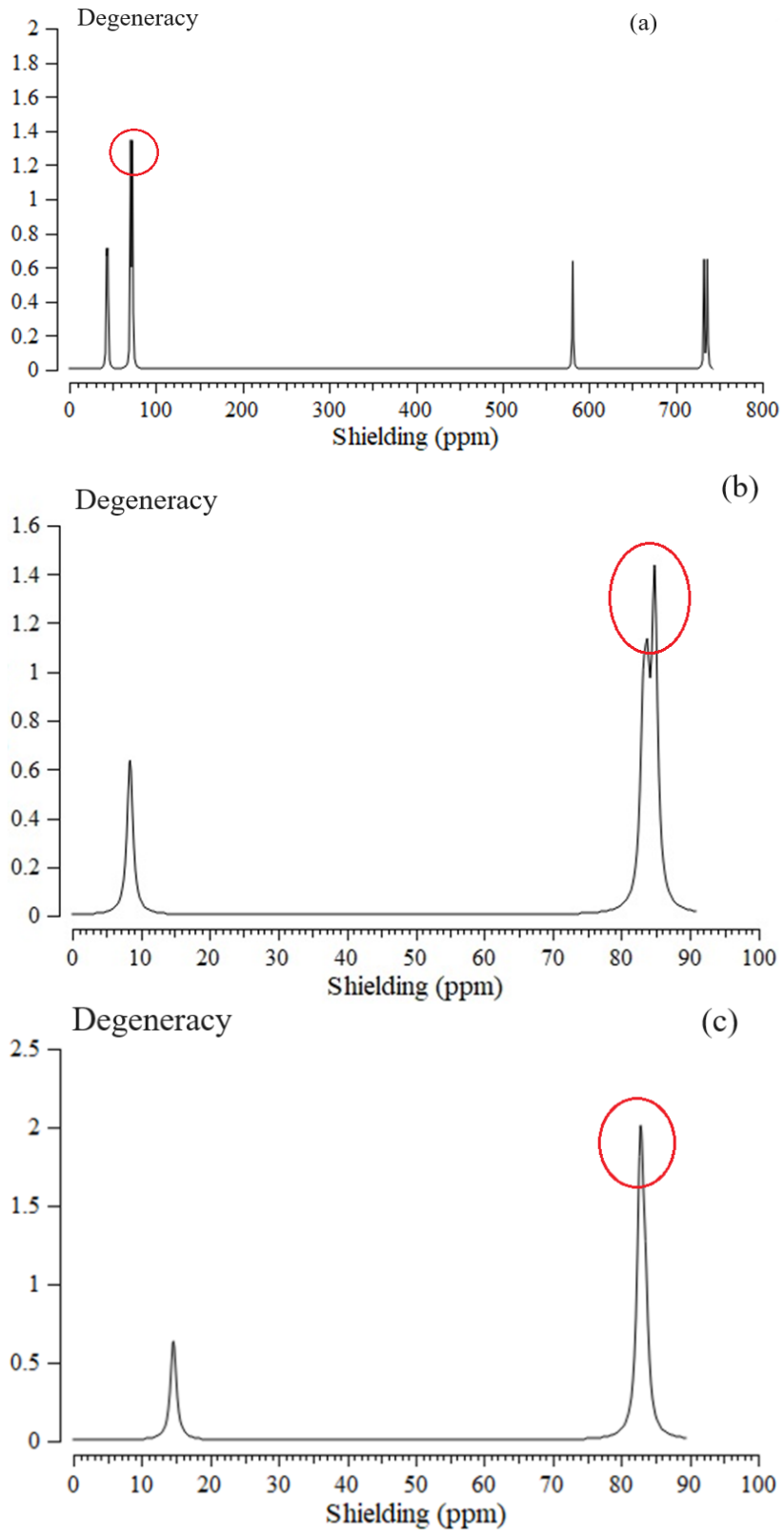


Figure 4: The NMR spectrums for (**a**) NO→Al–BN, (**b**) NO→C–BN, and (**c**) NO→Si–BN complexes.

2025, Vol. 1, Article ID. 2025.0005
https://www.doi.org/10.69709/MolModC.2025.339955

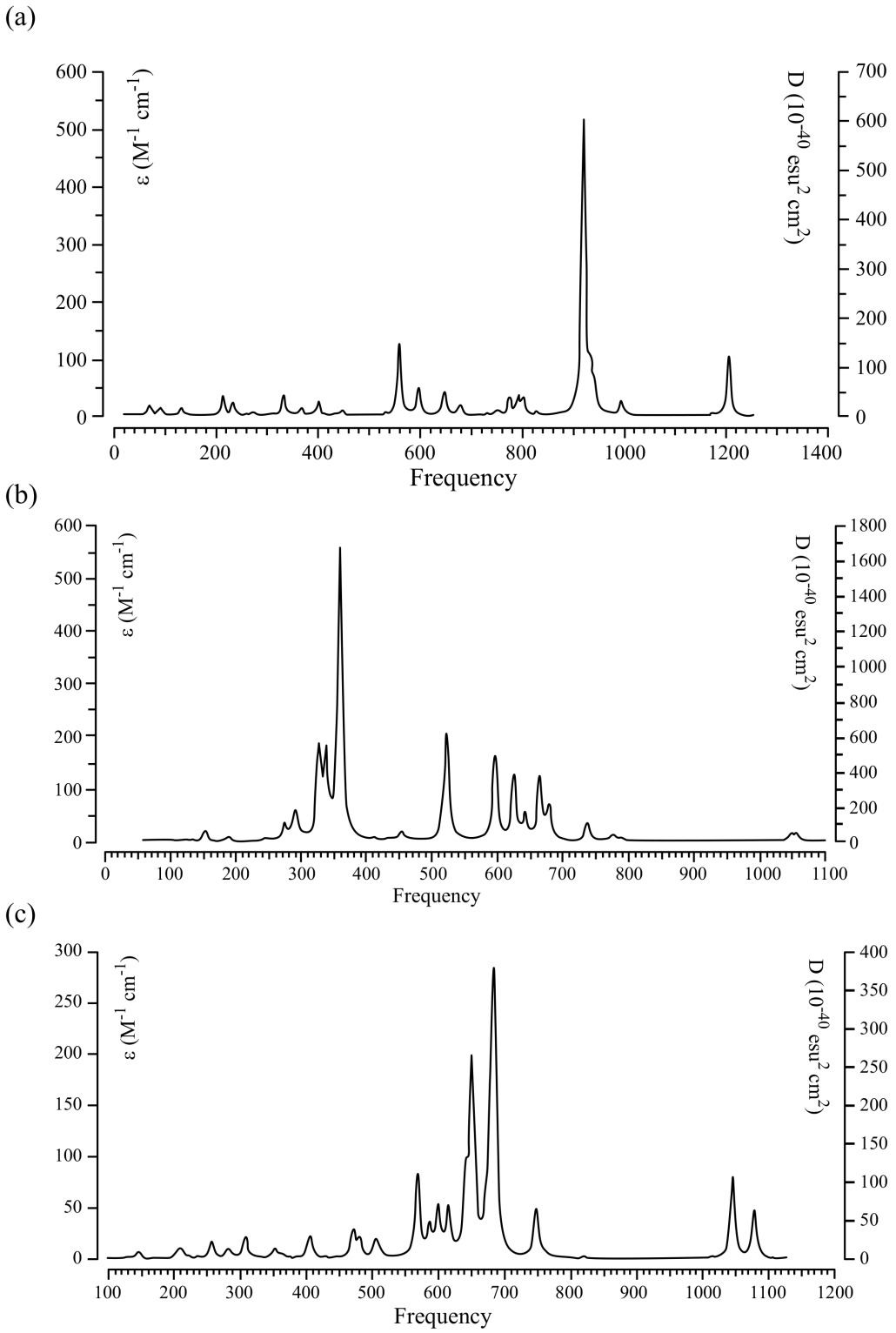


Figure 5: IR Frequency (cm^{-1}) spectra for (**a**) NO→Al–BN, (**b**) NO→C–BN, and (**c**) NO→Si–BN complexes.

References

[1] Gonzalez-Ortiz, D.; Salameh, C.; Bechelany, M.; Miele, P. Nanostructured boron nitride-based materials: Synthesis and applications. *Mater. Today Adv.* **2020**, *8*, 100107. [CrossRef]

[2] Mishra, N.S.; Saravanan, P. A review on the synergistic features of hexagonal boron nitride (white graphene) as adsorbent-photo active nanomaterial. *ChemistrySelect* **2018**, *3*, 8023–8034. [CrossRef]

[3] Weng, Q.H.; Wang, X.B.; Wang, X.; Bando, Y.; Golberg, D. Functionalized hexagonal boron nitride nanomaterials: Emerging properties and applications. *Chem. Soc. Rev.* **2016**, *45*, 3989–4012. [PubMed]

[4] Muñoz, A.D.O.; Escobedo-Morales, A.; Skakerzadeh, E.; Anota, E.C. Effect of homonuclear boron bonds in the adsorption of DNA nucleobases on boron nitride nanosheets. *J. Mol. Liq.* **2021**, *322*, 114951. [CrossRef]

[5] Shtansky, D.V.; Matveev, A.T.; Permyakova, E.S.; Leybo, D.V.; Konopatsky, A.S.; Sorokin, P.B. Recent Progress in Fabrication and Application of BN Nanostructures and BN-Based Nanohybrids. *Nanomaterials* **2022**, *12*, 2810. [CrossRef]

[6] Yang, Y.; Peng, Y.; Saleem, M.F.; Chen, Z.; Sun, W. Hexagonal Boron Nitride on III–V Compounds: A Review of the Synthesis and Applications. *Materials* **2022**, *15*, 4396. [CrossRef]

[7] Mollaamin, F. Features of Parametric Point Nuclear Magnetic Resonance of Metals Implantation on Boron Nitride Nanotube by Density Functional Theory/Electron Paramagnetic Resonance. *J. Comput. Theor. Nanosci.* **2014**, *11*, 2393–2398. [CrossRef]

[8] Bangari, R.S.; Yadav, V.K.; Singh, J.K.; Sinha, N. Fe_3O_4-functionalized boron nitride nanosheets as novel adsorbents for removal of arsenic(III) from contaminated water. *ACS Omega* **2020**, *5*, 10301–10314. [CrossRef]

[9] Chao, Y.H.; Zhang, J.; Li, H.P.; Wu, P.W.; Li, X.W.; Chang, H.H.; He, J.; Wu, H.F.; Li, H.M.; Zhu, W.S. Synthesis of boron nitride nanosheets with N-defects for efficient tetracycline antibiotics adsorptive removal. *Chem. Eng. J.* **2020**, *387*, 124138. [CrossRef]

[10] Vatanpour, V.; Mehrabani, S.A.N.; Keskin, B.; Arabi, N.; Zeytuncu, B.; Koyuncu, I. A comprehensive review on the applications of boron nitride nanomaterials in membrane fabrication and modification. *Ind. Eng. Chem. Res.* **2021**, *60*, 13391–13424. [CrossRef]

[11] Larki, S.; Shakerzadeh, E.; Anota, E.C.; Behjatmanesh-Ardakani, R. The Al, Ga and Sc dopants effect on the adsorption performance of B12N12 nanocluster toward pnictogen hydrides. *Chem. Phys.* **2019**, *526*, 110424. [CrossRef]

[12] Guo, Y.; Wang, R.X.; Wang, P.F.; Rao, L.; Wang, C. Developing a novel layered boron nitride-carbon nitride composite with high efficiency and selectivity to remove protonated dyes from water. *ACS Sustain. Chem.* **2019**, *7*, 5727–5741. [CrossRef]

[13] Chigo-Anota, E.; Escobedo-Morales, A.; Hernández-Cocoletzi, H.; López, J.G.L.Y. Nitric oxide adsorption on non-stoichiometric boron nitride fullerene: Structural stability, physicochemistry and drug delivery perspectives. *Phys. E: Low-Dimens. Syst. Nanostructures* **2015**, *74*, 538–543. [CrossRef]

[14] Shanaah, H.H.; Allangawi, A.; Usman, M.; Idrisov, E.; Ali, N.; Attique, S.; Hanif, M.B.; Mahmood, T.; Younis, A.; Iqbal, J. Cobalt-Doped Graphitic Carbon Nitride: A Multifunctional Material for Humidity Sensing, Electrochemical Water Splitting and Environmental Remediation Applications. *J. Alloys Compd.* **2024**, *1008*, 176498. [CrossRef]

[15] Younis, A.; Sehar, S.; Guan, X.; Aftab, S.; Manaa, H.; Mahmood, T.; Iqbal, J.; Akram, F.; Ali, N.; Wu, T. Four-in-one strategy to boost the performance of 3-dimensional MoS_2 nanostructures for industrial effluent treatment and hydrogen evolution reactions. *J. Alloys Compd.* **2024**, *976*, 173104. [CrossRef]

[16] Tariq, F.; Malik, Y.; Naseem, N.; Zahid, W.A.; Younis, A.; Kher, R.A.; Ayub, K.; Iqbal, J. Sensing Potential of Carbon Nitride (C_6N_8) for the Detection of Hydrogen Sulfide (H_2S) and Nitrogen Trichloride (NCl_3): A DFT Approach. *IEEE Sens. J.* **2024**, *24*, 9383–9389. [CrossRef]

[17] Abdullah; Rasheed, A.; Younis, A.; Khan, M.A. Wearable Piezoelectric BioMEMS-based Sensor for SARS-CoV-2 (COVID-19) Virus Droplets Detection. In Proceedings of the IEEE 15th International Conference on Nano/Molecular Medicine & Engineering (NANOMED), Taipei, Taiwan, 15–17 November 2021. [CrossRef]

[18] Younis, A.; Loucif, A. Defects mediated enhanced catalytic and humidity sensing performance in ceria nanorods. *Ceram. Int.* **2021**, *47*, 15500–15507. [CrossRef]

[19] Henkelman, G.; Arnaldsson, A.; Jónsson, H. A fast and robust algorithm for Bader decomposition of charge density. *Comput. Mater. Sci.* **2006**, *36*, 354–360. [CrossRef]

[20] Blöchl, P.E. Projector augmented-wave method. *Phys. Rev. B* **1994**, *50*, 17953–17979. [CrossRef]

[21] Perdew, J.P.; Burke, K.; Ernzerhof, M. Generalized gradient approximation made simple. *Phys. Rev. Lett.* **1996**, *77*, 3865. [CrossRef]

[22] Ziesche, P.; Kurth, S.; Perdew, J.P. Density functionals from LDA to GGA. *Comput. Mater. Sci.* **1998**, *11*, 122–127. [CrossRef]

[23] Arrigoni, M.; Madsen, G.K.H. Comparing the performance of LDA and GGA functionals in predicting the T lattice thermal conductivity of III-V semiconductor materials in the zincblende structure: The cases of AlAs and BAs. *Comput. Mater. Sci.* **2019**, *156*, 354–360. [CrossRef]

[24] Hohenberg, P.; Kohn, W. Inhomogeneous Electron Gas. *Phys. Rev. B* **1964**, *136*, B864–B871. [CrossRef]

[25] Kohn, W.; Sham, L.J. Self-Consistent Equations Including Exchange and Correlation Effects. *Phys. Rev.* **1965**, *140*, A1133–A1138. [CrossRef]

[26] Becke, A.D. Density-functional thermochemistry. III. The role of exact exchange. *J. Chem. Phys.* **1993**, *98*, 5648–5652. [CrossRef]

[27] Lee, C.; Yang, W.; Parr, R.G. Development of the Colle–Salvetti correlation-energy formula into a functional of the electron density. *Phys. Rev. B* **1988**, *37*, 785–789. [CrossRef]

[28] Kim, K.; Jordan, K.D. Comparison of Density Functional and MP2 Calculations on the Water Monomer and Dimer. *J. Phys. Chem.* **1994**, *98*, 10089–10094. [CrossRef]

[29] Stephens, P.J.; Devlin, F.J.; Chabalowski, C.F.; Frisch, M.J. Ab Initio Calculation of Vibrational Absorption and Circular Dichroism Spectra Using Density Functional Force Fields. *J. Phys. Chem.* **1994**, *98*, 11623–11627. [CrossRef]

[30] Cramer, C.J. Essentials of Computational Chemistry: Theories and Models, 2nd Edition Wiley. 2004. Available online: https://www.wiley.com/en-cn (accessed on 24 June 2021).

[31] Mollaamina, F.; Mohammadi, S.; Khalaj, Z.; Monajjemi, M. Computational Modelling of Boron Nitride Nanosheet for Detecting and Trapping of Water Contaminant. *Russ. J. Phys. Chem. B* **2024**, *18*, 67–82. [CrossRef]

[32] Mollaamin, F.; Monajjemi, M. In Situ Ti-Embedded SiC as Chemiresistive Nanosensor for Safety Monitoring of CO, CO_2, NO, NO_2: Molecular Modelling by Conceptual Density Functional Theory. *Russ. J. Phys. Chem. B* **2024**, *18*, 49–66. [CrossRef]

[33] Vosko, S.H.; Wilk, L.; Nusair, M. Accurate spin-dependent electron liquid correlation energies for local spin density calculations: A critical analysis. *Can. J. Phys.* **1980**, *58*, 1200–1211. [CrossRef]

[34] Frisch, M.J.; Trucks, G.W.; Schlegel, H.B.; Scuseria, G.E.; Robb, M.A.; Cheeseman, J.R.; Scalmani, G.; Barone, V.; Petersson, G.A.; Nakatsuji, H.; et al. *Gaussian 16, Revision C.01*; Gaussian, Inc.: Wallingford, CT, USA, 2016. [Google Scholar]

[35] Dennington, R.; Keith, T.A.; Millam, J.M. *GaussView, Version 6.06.16*; Semichem Inc.: Shawnee Mission, KS, USA, 2016. [Google Scholar]

[36] Monajjemi, M.; Mahdavian, L.; Mollaamin, F.; Khaleghian, M. Interaction of Na, Mg, Al, Si with carbon nanotube (CNT): NMR and IR study. *Russ. J. Inorg. Chem.* **2009**, *54*, 1465–1473. [CrossRef]

[37] Bakhshi, K.; Mollaamin, F.; Monajjemi, M. Exchange and Correlation Effect of Hydrogen Chemisorption on Nano V(100) Surface: A DFT Study by Generalized Gradient Approximation (GGA). *J. Comput. Theor. Nanosci.* **2011**, *8*, 763–768. [CrossRef]

[38] Khaleghian, M.; Zahmatkesh, M.; Mollaamin, F.; Monajjemi, M. Investigation of Solvent Effects on Armchair Single-Walled Carbon Nanotubes: A QM/MD Study. *Fuller. Nanotub. Carbon. Nanostruct* **2011**, *19*, 251–261. [CrossRef]

[39] Mollaamin, F.; Monajjemi, M. Harmonic Linear Combination and Normal Mode Analysis of Semiconductor Nanotubes Vibrations. *J. Comput. Theor. Nanosci.* **2015**, *12*, 1030–1039. [CrossRef]

[40] Zadeh, M.A.A.; Lari, H.; Kharghanian, L.; Balali, E.; Khadivi, R.; Yahyaei, H.; Mollaamin, F.; Monajjemi, M. Density functional theory study and anti-cancer properties of shyshaq plant: In view point of nano biotechnology. *J. Comput. Theor. Nanosci.* **2015**, *12*, 4358–4367. [CrossRef]

[41] Monajjemi, M.; Baie, M.T.; Mollaamin, F. Interaction between threonine and cadmium cation in [Cd(Thr)] (n = 1–3) complexes: Density functional calculations. *Russ. Chem. Bull.* **2010**, *59*, 886–889. [CrossRef]

[42] Monajjemi, M.; Khaleghian, M.; Tadayonpour, N.; Mollaamin, F. The effect of different solvents and temperatures on stability of single-walled carbon nanotube: A QM/MD study. *Int. J. Nanosci.* **2010**, *09*, 517–529. [CrossRef]

[43] Tahan, A.; Mollaamin, F.; Monajjemi, M. Thermochemistry and NBO analysis of peptide bond: Investigation of basis sets and binding energy. *Russ. J. Phys. Chem. A* **2009**, *83*, 587–597. [CrossRef]

[44] Mollaamin, F.; Monajjemi, M. Trapping of toxic heavy metals from water by GN–nanocage: Application of nanomaterials for contaminant removal technique. *J. Mol. Struct.* **2024**, *1300*, 137214. [CrossRef]

[45] Mollaamin, F.; Ilkhani, A.; Sakhaei, N.; Bonsakhteh, B.; Faridchehr, A.; Tohidi, S.; Monajjemi, M. Thermodynamic and solvent effect on dynamic structures of nano bilayer-cell membrane: Hydrogen bonding study. *J. Comput. Theor. Nanosci.* **2015**, *12*, 3148–3154. [CrossRef]

[46] Mollaamin, F.; Majid Monajjemi, M. Hexagonal Honeycomb Pl-Gan Nanosheet as Adsorbent Surface for Gas Molecules Sensing: A Quantum Chemical Study. *Surf. Rev. Lett. (SRL)* **2024**, *31*, 1–14. [CrossRef]

[47] Khalili Hadad, B.; Mollaamin, F.; Monajjemi, M. Biophysical chemistry of macrocycles for drug delivery: A theoretical study. *Russ. Chem. Bull.* **2011**, *60*, 238–241. [CrossRef]

[48] Mollaamin, F.; Shahriari, S.; Monajjemi, M.; Khalaj, Z. Nanocluster of Aluminum Lattice via Organic Inhibitors Coating: A Study of Freundlich Adsorption. *J. Clust. Sci.* **2023**, *34*, 1547–1562. [CrossRef]

[49] Mollaamin, F.; Monajjemi, M. Electric and Magnetic Evaluation of Aluminum–Magnesium Nanoalloy Decorated with Germanium Through Heterocyclic Carbenes Adsorption: A Density Functional Theory Study. *Russ. J. Phys. Chem. B* **2023**, *17*, 658–672. [CrossRef]

[50] Mollaamin, F.; Monajjemi, M. Adsorption ability of Ga_5N_{10} nanomaterial for removing metal ions contamination from drinking water by DFT. *Int. J. Quantum Chem.* **2024**, *124*, e27348. [CrossRef]

[51] Mollaamin, F.; Monajjemi, M. Molecular modelling framework of metal-organic clusters for conserving surfaces: Langmuir sorption through the

TD-DFT/ONIOM approach. *Mol. Simul.* **2023**, *49*, 365–376. [CrossRef]

[52] Mollaamin, F.; Monajjemi, M.; Salemi, S.; Baei, M.T. A Dielectric Effect on Normal Mode Analysis and Symmetry of BNNT Nanotube. *Fuller. Nanotub. Carbon. Nanostructures* **2011**, *19*, 182–196. [CrossRef]

[53] Sarasia, E.M.; Afsharnezhad, S.; Honarparvar, B.; Mollaamin, F.; Monajjemi, M. Theoretical study of solvent effect on NMR shielding tensors of luciferin derivatives. *Phys. Chem. Liq.* **2011**, *49*, 561–571. [CrossRef]

[54] Shahriari, S.; Mollaamin, F.; Monajjemi, M. Increasing the Performance of {[(1-x-y) $LiCo_{0.3}Cu_{0.7}$] (Al and Mg doped)] O_2}, xLi_2MnO_3, $yLiCoO_2$ Composites as Cathode Material in Lithium-Ion Battery: Synthesis and Characterization. *Micromachines* **2023**, *14*, 241. [CrossRef]

[55] Monajjemi, M.; Mollaamin, F.; Shojaei, S. An overview on Coronaviruses family from past to Covid-19: Introduce some inhibitors as antiviruses from Gillan's plants. *Biointerface Res. Appl. Chem.* **2020**, *10*, 5575. [CrossRef]

[56] Mollaamin, F.; Monajjemi, M. Tailoring and functionalizing the graphitic-like GaN and GaP nanostructures as selective sensors for NO, NO_2, and NH_3 adsorbing: A DFT study. *J. Mol. Model.* **2023**, *29*, 170. [CrossRef]

[57] Mollaamin, F.; Monajjemi, M. In Silico-DFT Investigation of Nanocluster Alloys of Al-(Mg, Ge, Sn) Coated by Nitrogen Heterocyclic Carbenes as Corrosion Inhibitors. *J. Clust. Sci.* **2023**, *34*, 2901–2918. [CrossRef]

[58] Mollaamin, F.; Monajjemi, M. Transition metal (X = Mn, Fe, Co, Ni, Cu, Zn)-doped graphene as gas sensor for CO_2 and NO_2 detection: A molecular modeling framework by DFT perspective. *J. Mol. Model.* **2023**, *29*, 119. [CrossRef] [PubMed]

[59] Mollaamin, F.; Monajjemi, M. Graphene-based resistant sensor decorated with Mn, Co, Cu for nitric oxide detection: Langmuir adsorption & DFT method. *Sens. Rev.* **2023**, *43*, 266–279. [CrossRef]

[60] Meng, Y.S.; Dompablo, M.E.A.-D. First principles computational materials design for energy storage materials in lithium ion batteries. *Energy Environ. Sci.* **2009**, *2*, 589–609. [CrossRef]

[61] Yanai, T.; Tew, D.P.; Handy, N.C. A new hybrid exchange–correlation functional using the Coulomb-attenuating method (CAM-B3LYP). *Chem. Phys. Lett.* **2004**, *393*, 51–57. [CrossRef]

[62] Grimme, S.; Antony, J.; Ehrlich, S.; Krieg, H. A consistent and accurate ab initio parametrization of density functional dispersion correction (DFT-D) for the 94 elements H-Pu. *J. Chem. Phys.* **2010**, *132*, 154104. [CrossRef]

[63] Trontelj, Z.; Pirnat, J.; Jazbinšek, V.; Lužnik, J.; Srčič, S.; Lavrič, Z.; Beguš, S.; Apih, T.; Žagar, V.; Seliger, J. Nuclear Quadrupole Resonance (NQR)—A Useful Spectroscopic Tool in Pharmacy for the Study of Polymorphism. *Crystals* **2020**, *10*, 450. [CrossRef]

[64] Sciotto, R.; Ruiz Alvarado, I.A.; Schmidt, W.G. Substrate Doping and Defect Influence on P-Rich InP(001):H Surface Properties. *Surfaces* **2024**, *7*, 79–87. [CrossRef]

[65] Luo, J.; Wang, C.; Wang, Z.; Guo, Q.; Yang, J.; Rui Zhou, R.; Matano, K.; Oguchi, T.; Ren, Z. NMR and NQR studies on transition-metal arsenide superconductors $LaRu_2As_2$, $KCa_2Fe_4As_4F_2$, and $A_2Cr_3As_3$. *Chin. Phys. B* **2020**, *29B*, 067402. [CrossRef]

[66] Young, H.A.; Freedman, R.D. *Sears and Zemansky's University Physics with Modern Physics*, 13th ed.; Addison-Wesley: Boston, MA, USA, 2012; p. 754.